



## Research article

Development of microcrystalline cellulose based hydrogels for the *in vitro* delivery of Cephalexin

Debashis Kundu, Tamal Banerjee \*

Department of Chemical Engineering, Indian Institute of Technology Guwahati, Guwahati, Assam, 781039, India

## ARTICLE INFO

## Keywords:

Chemical Engineering  
 Biochemical Engineering  
 Chemical synthesis  
 Drug delivery  
 Rheology  
 Biomaterials  
 Hydrogel  
 Microcrystalline cellulose  
 Cephalexin

## ABSTRACT

Three hydrogels namely, microcrystalline cellulose (MCC), microcrystalline cellulose-carboxymethyl cellulose (MCC-CMC) and microcrystalline cellulose-xylan (MCC-xylan) are synthesized using ethylene glycol diglycidyl ether as crosslinker. For the chemical characterization, FT-IR spectroscopy is adopted, whereas gel fraction and swelling ratio are used for the physical characterization of the hydrogels. Coarse morphology of hydrogels is further visualized by microscopic observation. The rheological characterization proves that MCC-CMC gel withstands higher strain to resist permanent deformation than the other two gels. The hydrogels are used for the loading and *in vitro* release of Cephalexin. The *in vitro* delivery is carried out in various simulated body fluids such as phosphate buffer saline (PBS), artificial intestinal fluid (AIF) and artificial gastric fluid (AGF). MCC-CMC is observed to deliver Cephalexin individually 15% in AGF, 86% in AIF, 98% in PBS and 98% in consecutive buffers (AGF followed by AIF and PBS).

## 1. Introduction

Cellulose is a natural biopolymer with a linearly ordered  $\beta$ -(1 $\rightarrow$ 4)-linked D-anhydrogluco pyranose repeating units and found in plants, bacteria, fungi and sea animals [1]. A prominent class of cellulose is microcrystalline cellulose (MCC) which is prepared by the treatment of alpha cellulose with excess amount of mineral acids. It has a reduced degree of polymerization ( $\sim$ 100) and hence possesses shorter polymeric chains. MCC has characteristic properties such as non-toxicity, high mechanical strength, low density, large surface area, biodegradability and biocompatibility. The fascinating mechanical and chemical properties drew attention from scientific community as well as various industries. MCC is widely used as thickeners, binders and adsorbents in pharmaceutical and cosmetic industries; gelling agents, stabilizers and anticaking agents in food and beverage industries [2]. In addition to the advantages, MCC suffers drawback due to incompatibility with most polymeric matrices, poor wettability, insolubility in organic and aqueous medium due to inherent crystallinity. In order to overcome this barrier, various solvents such as deep eutectic solvent, ionic liquid and alkali/urea systems are used to solubilize MCC [3]. The various strategies of solubilization of MCC open up the possibility of forming hydrogels from MCC.

Hydrogels are three dimensional polymeric network crosslinked either physically or chemically. The network swells upon absorbing large amount of water. Synthetic or natural polymers possessing biocompatibility are used as hydrogel forming material. High retention capacity of water and interconnected three dimensional network mimic the extracellular matrix. This property makes them a vital clog in biomedical applications, tissue engineering, delivery of drugs and proteins [4]. The inherent insoluble nature limits MCC as hydrogel precursor. Choe et al. reported pure MCC based hydrogel after dissolving it in tetrabutylammonium fluoride/dimethyl sulfoxide solvent and subsequent adjustment in viscosity [5]. Conductive hydrogel is also being reported by dissolving MCC in ionic liquid and further aided by polypyrrole [6]. Thiol-ene click chemistry based MCC hydrogels are prepared by exposing the allyl functionalized MCC into UV exposure [7].

The water soluble derivative of cellulose such as carboxymethyl cellulose (CMC) is widely used as precursor for hydrogel. It is synthesized by substituting hydrogen atom of D-glucopyranose ring with carboxymethyl moiety. Apart from biocompatible and pH sensitive hydrogels, CMC is used in food products (as thickener and emulsion stabilizer), non-food products (as diet pills, tooth pastes, laxatives, water based paints, paper products etc.) and biomedical fields [8]. Hemicellulose is heteropolysaccharide, flexible, amorphous and second most abundant material

\* Corresponding author.

E-mail address: [tamalb@iitg.ac.in](mailto:tamalb@iitg.ac.in) (T. Banerjee).

found in woods after cellulose and possesses lower degree of polymerization (~200 residues) than cellulose. Xylan is most abundant form of hemicellulose and consists  $\beta$ -(1→4)-D-xylopyranose units as backbone. The gel and film forming properties of hemicellulose coupled with its biocompatibility and biodegradability nature finds application in biomedical applications, drug delivery and as adhesive, coating and additive in pharmacy and food industries [9]. Additionally, multiple stimuli, such as organic solvent, ion, pH sensitive xylan-based gels have gained recent attention [10]. Due to this property, the xylan based hydrogels have been used as a carrier for drugs and biological macromolecules [11], biosorbent for organic dyes and metal ions [12, 13].

Cephalexin is first generation cephalosporin drug which belongs to lactam antibiotics and possess similar fundamental structural requirements like penicillin. It is a semisynthetic antibiotic derived from cephalosporin and is almost completely absorbed from the gastrointestinal tract with a bioavailability of 95% [14]. The half-life of Cephalexin is approximately 1.1 h and prescribed 3–4 times a day to maintain therapeutic range [15]. The structure of the molecule is similar to acid-base molecule because of the presence of  $-\text{NH}_2$ ,  $-\text{CONH}$  and  $-\text{COOH}$  moieties. Cephalosporins are the commonly prescribed antibiotics which are considered as the safest and most effective broad spectrum bactericidal antimicrobial agents [15]. By inhibiting the synthesis of essential structural components of bacterial cell wall, they prevent the infection due to gram-positive and gram-negative bacteria. Hence studies concerning its release need to be undertaken in various environments. Being an antibiotic drug, the essence of efficient delivery of it using carrier is an important aspect. The controlled delivery in scheduled time will reduce the dosage of the drug and hence reduces the possible side effects. Hydrogel is proved to be important carrier for various drugs. Limited studies of release of Cephalexin by hydrogels are being reported in the literature. The Cephalexin delivery of hydrogel formed by 2-hydroxyethyl methacrylate, itaconic acid and poly (alkylene glycol) methacrylates is reported by Tomić et al [16]. Barkhordari and Yadollahi reported enhanced protection and controlled liberation of Cephalexin drug in gastrointestinal tract using CMC encapsulated layered double hydroxides-drug nanohybrids [14].

In this current work, we have synthesized three hydrogels namely MCC gel, MCC-CMC gel and MCC-xylan gel using ethylene glycol diglycidyl ether (EGDE) as crosslinker. The difunctional EGDE has two epoxide rings at both ends. The highly strained epoxy rings open up at high alkaline pH and react with the hydroxyl and carboxymethyl moieties to form crosslinked structure [17]. The EGDE crosslinker is popularly used for  $\beta$ -cyclodextrin-polysaccharide [18],  $\beta$ -cyclodextrin-poly(vinyl)alcohol [19], gelatin and chitosan [20] based hydrogels. MCC has not been explored as precursor of hydrogel as that of other derivatives of cellulose. The biocompatible solubilization technique using aqueous sodium hydroxide (NaOH)/urea solvent and subsequent copolymerization with CMC and xylan create novel kind of polysaccharide based hydrogels. The characterization methods include Fourier Transform Infra-Red (FT-IR) spectroscopy, gel fraction and swelling ratio. The morphology of the gels is viewed in field emission scanning electron microscope (FESEM) and optical microscope. Rheology of the hydrogel is further measured at 25 °C in a cone and plate rheometer. The MCC based gels are loaded with model drug namely, Cephalexin and the *in vitro* delivery of Cephalexin is carried out in various simulated body fluids such as artificial gastric fluid (AGF), artificial intestinal fluid (AIF) and phosphate buffer saline (PBS).

## 2. Materials and methods

### 2.1. Materials

Beachwood xylan, Carboxymethyl cellulose sodium salt were procured from Sigma Aldrich. Microcrystalline cellulose was purchased from Merck. Sodium chloride, urea, sodium hydroxide, hydrochloric acid (37 wt%) (HCl) and potassium dihydrogen phosphate were procured from

Merck. PBS was procured from Himedia. Ethylene glycol diglycidyl ether and Cephalexin monohydrate were procured from TCI India. The chemicals were of analytical grade and used in as received condition. The in-house water purification facility (make: Millipore, model: ELix-3) was used as source of deionized (DI) water.

### 2.2. Preparation of hydrogels

An aqueous solution containing 40 wt% urea and 60 wt% NaOH, was used to dissolve MCC [21]. Separately, 1 mol L<sup>-1</sup> aqueous sodium hydroxide solution was used to dissolve xylan and CMC. CMC and xylan solutions were independently mixed with MCC solution in 1:1 molar ratio to prepare MCC-CMC and MCC-xylan precursor solutions. The homogeneous solution is obtained after heating the mixture to 50 °C. Next, the EGDE crosslinker was added drop wise into the homogeneous mixture. Pure MCC gel was synthesized by adding EGDE drop wise into the MCC solution. The gelation process was understood to complete within 20 min. Thereafter, the gel was transferred to a beaker and allowed to swell in DI water. The subsequent swelling removed the excess unreacted precursor from the gel. The gel was kept in the DI water for 48 h, refreshing the water six times daily. The removal of excess precursor is an essential step, since the unreacted precursor will leach out from the crosslinked hydrogel matrix. Thereafter, 0.1 M HCl solution was used to remove the excess amount of NaOH and hereby neutralization of pH. The pH neutral gel was later lyophilized (make: Martin Christ, model: Alpha 2–4 LD) for further characterization. The reaction scheme of all three hydrogels is given in Figure 1.

### 2.3. Characterization

#### 2.3.1. FT-IR spectroscopy

Excess amount of dried potassium bromide was mixed with freeze dried hydrogel. Therefore, the transparent pellet was formed by pressing the powder inside a pellet press. The FT-IR spectra of the pellets were recorded from 400 cm<sup>-1</sup> to 4000 cm<sup>-1</sup> with a resolution of 4 cm<sup>-1</sup> and using 30 scans per sample in FT-IR spectrometer (make: Shimadzu, model: IRAffinity-1).

#### 2.3.2. Morphology

The morphology of freeze dried hydrogels was visualized in optical microscope (make: Carl Zeiss, model: Scope A1, AXIO, software: ZEN 2.3) and FESEM (make: Carl Zeiss, model: GeminiSEM 300). Gold coated freeze dried hydrogel, was taken for FESEM visualization with an optical zoom of 200 nm and 1  $\mu\text{m}$  and a potential of 3 kV. Freeze dried hydrogel was placed on a glass slide covering with coverslip to snap the optical microscopic images.

#### 2.3.3. Rheology

The rheological measurement on developed hydrogels were performed in a rheometer (make: Anton Paar (Austria), model: Physica MCR 301) employing a cone and plate geometry (diameter: 50 mm, angle: 1°, 0.1 mm gap) at 25 °C. The viscosity of the synthesized gels was measured between shear rates of 0.01–1000 s<sup>-1</sup>. The amplitude sweep tests were performed with a strain of 0.1–1000% range and with a constant angular frequency of 1 Hz. The amplitude sweep test determines the storage moduli ( $G'$ ), loss moduli ( $G''$ ) and linear viscoelastic region profiles (LVR). The crossover point is defined as the intersection point of  $G'$  and  $G''$ . After obtaining the LVR, frequency sweep test was carried out within a frequency of 0.01–100 Hz and at constant strain of 5%. The loss tangent ( $\tan \delta$ ) is defined as the ratio of loss moduli to storage moduli and is given as,

$$\tan \delta = \frac{G''}{G'} \quad (1)$$

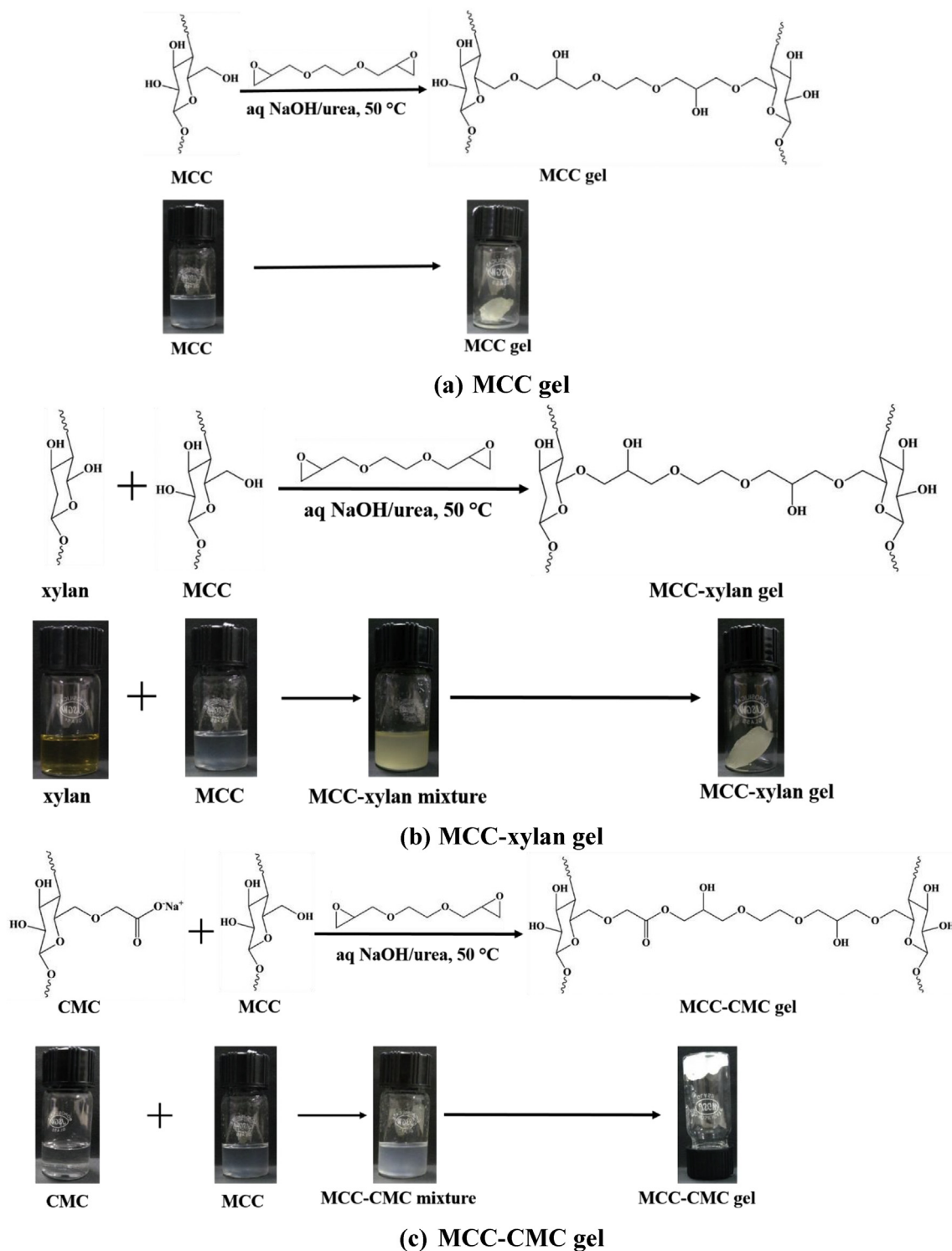


Figure 1. Reaction scheme of hydrogel formation. (a) MCC gel, (b) MCC-xylan gel, (c) MCC-CMC gel.

#### 2.3.4. Preparation of AGF and AIF

AGF and AIF were prepared as outlined by Gao et al. [22]. Briefly, 2 gm of sodium chloride and 7 mL of HCl (37 wt%) were dissolved in water in 1 L volumetric flask. The pH of solution was adjusted to 1.2 after adjusting the total volume to 1 L. The 1 L AIF solution was prepared by dissolving 6.8 gm of potassium dihydrogen phosphate and adjustment of pH to 6.8. The pH of solutions was measured by digital pH meter (make: Eutech Instruments, model: EUTECH pH700).

#### 2.3.5. Equilibrium swelling ratio

The swelling of hydrogel was measured in AGF (pH = 1.2), AIF (pH = 6.8) and PBS (pH = 7.4) along with DI water. A measured amount of dried hydrogel ( $W_d$ , gm) was immersed in buffers and DI water for 48 h at 25 °C. After equilibrium is reached, the excess water was removed from the swollen hydrogel by filtration. Thereafter the equilibrium weight of hydrogels ( $W_{eq}$ ) was measured. The equilibrium swelling ratio (SR) is measured by the following formula:

$$SR(\%) = \frac{(W_{eq} - W_i)}{W_i} \times 100\% \quad (2)$$

### 2.3.6. Gel fraction

The constant weight of hydrogel ( $W_0$ ) was measured after drying at 60 °C for 24 h. Thereafter the hydrogel was submerged in DI water to remove the soluble parts and subsequently heated at 121 °C for 4 h. In the next step, the hydrogel was dried at 60 °C for 72 h with subsequent measurement of weight ( $W_1$ ). The gel fraction is then given by [23],

$$gel\ fraction(\%) = \left(\frac{W_1}{W_0}\right) \times 100\% \quad (3)$$

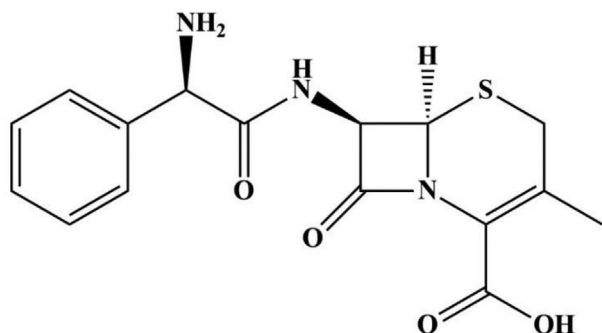


Figure 2. Chemical structure of Cephalexin [14].

Both the measurement of gel fraction and equilibrium swelling ratio were triplicated and the error bars represent the standard deviation of measurement.

### 2.4. Loading of Cephalexin

Cephalexin is used as model drug to study the loading and *in vitro* release of drug at different physiological buffers. The structure of Cephalexin is given in Figure 2. Freeze dried hydrogel was submerged in 20 mL Cephalexin ( $0.5\text{ mg mL}^{-1}$ ) solution and kept inside an orbital shaker at 120 rpm and 25 °C ( $\pm 0.5$  °C) for 48 h. After 48 h, clear supernatant was obtained by placing the tubes in centrifuge at 10,000 rpm. Thereafter the samples were filtered to separate the supernatant and drug loaded gels. Later, the drug loaded gels were lyophilized. The concentration of Cephalexin in supernatant was measured against the absorbance values obtained from UV-vis spectrophotometer. The percent amount of loaded drug into the hydrogel (drug loading) is given by [24],

$$Drug\ loading(\%) = \frac{\text{Amount of drug in hydrogel}}{\text{Amount of freeze dried hydrogel}} \times 100 \quad (4)$$

### 2.5. *In vitro* release of Cephalexin

20 mL of AGF, AIF and PBS buffer solutions were added separately in the Cephalexin loaded hydrogels. The sample tubes were kept inside orbital shaker at 37 °C ( $\pm 0.5$  °C) and 60 rpm. At a definite interval, 5 mL aliquot was collected and subsequently 5 mL fresh buffer solution was

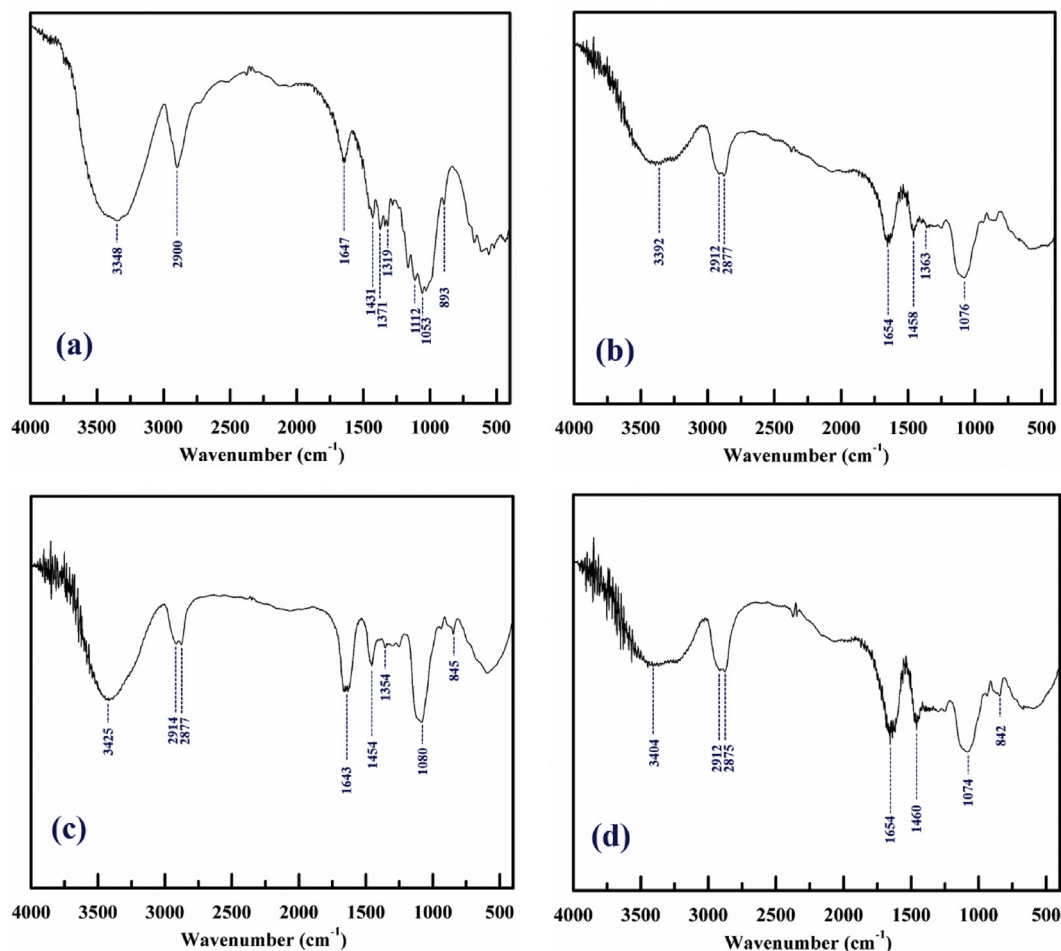


Figure 3. FT-IR spectra, (a) MCC pure, (b) MCC gel, (c) MCC-CMC, (d) MCC-xylan.



added to make up the volume. The collection method of aliquot is adopted from literature [25]. The absorbance of aliquots is measured in UV-vis spectrophotometer and corresponding concentration was calculated against calibration curve. The fraction of Cephalexin release at any certain time ( $F_t$ ) is given by,

$$F_t(\%) = \frac{M_t}{M_0} \times 100 \quad (5)$$

Where,  $M_t$  is the amount of Cephalexin release from hydrogel at a certain time and  $M_0$  is the total amount of Cephalexin loaded initially. All release experiments were performed three times and the standard deviations are reported as error bars in the release profiles.

### 2.6. UV-vis spectroscopy

UV-vis spectrophotometer (make: Shimadzu, model: UV-2600) was used to measure the absorbance of supernatant solutions and aliquots. The concentration of Cephalexin in aliquots and supernatant solutions was calculated from the absorbance values using calibration curve. Stock Cephalexin solution ( $1 \text{ mg mL}^{-1}$ ) was appropriately diluted to prepare the known concentrations. The calibration curve was prepared from absorbance data of known Cephalexin concentrations. Independent calibration curves were prepared for DI water (for supernatant) and AGF, AIF, PBS buffers (for the aliquots).

## 3. Results and discussions

### 3.1. Fourier transform infrared spectra

The Fourier Transform Infrared spectra of pure MCC, MCC gel, MCC-CMC and MCC-xylan are given in Figure 3. The monomers consist of pyranose ring having characteristic stretching peak of O-H, C-H, C-O and bending of C-H, C-C. Additionally it has skeletal vibration of C-O and C-C in the pyranose ring and the C-H glycosidic deformation and antisymmetric  $\beta$ -(1 $\rightarrow$ 4) glycosidic linkage. Figure 3a represents FT-IR spectra of pure MCC. The O-H and C-H stretching are assigned at  $3348 \text{ cm}^{-1}$  and  $2900 \text{ cm}^{-1}$  respectively. The characteristic peak at  $1431 \text{ cm}^{-1}$  is assigned as bending of  $-\text{CH}_2$ . The skeletal vibrations are recorded at  $1371 \text{ cm}^{-1}$ . The antisymmetric  $\beta$ -(1 $\rightarrow$ 4) glycosidic linkage is reported at  $1090 \text{ cm}^{-1}$  [26] while the bending of C-C is reported at  $1064 \text{ cm}^{-1}$  [17]. Here, we observe minor shift in antisymmetric  $\beta$ -(1 $\rightarrow$ 4) glycosidic linkage and is assigned at  $1112 \text{ cm}^{-1}$ . The C-C bending is assigned at  $1053 \text{ cm}^{-1}$ . The band at  $893 \text{ cm}^{-1}$  is assigned as C-H glycosidic deformation with ring vibration.

The FT-IR spectra of MCC gel, MCC-CMC, MCC-xylan are given in Figure 3b-d. The characteristic peaks are found in similar positions for all three gels. The O-H stretching is assigned at  $3392\text{-}3425 \text{ cm}^{-1}$ . The doublet peaks at  $2912\text{-}2914 \text{ cm}^{-1}$  and  $2875\text{-}2877 \text{ cm}^{-1}$  are assigned for C-H stretching and bending respectively. The peak at  $1454\text{-}1460 \text{ cm}^{-1}$  represents bending of  $-\text{CH}_2$ , which is present both in monomers and

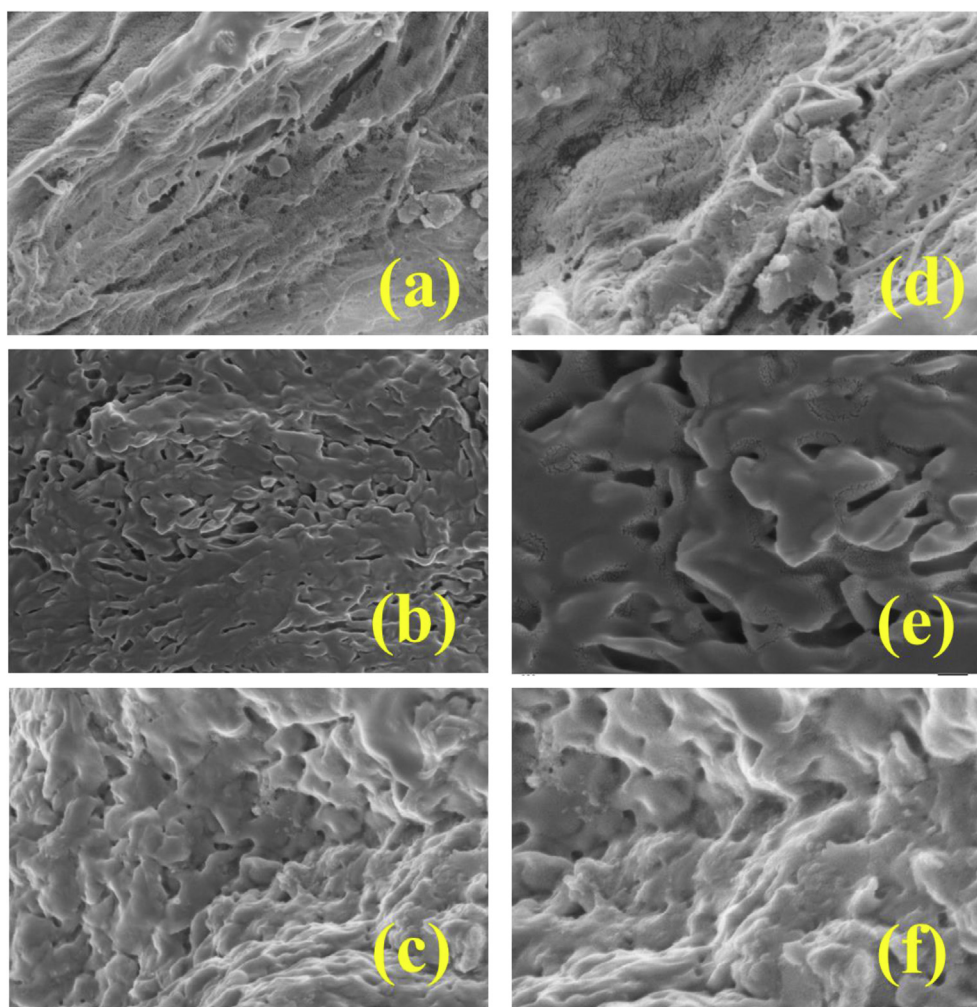


Figure 4. FESEM morphology of hydrogels at  $1 \mu\text{m}$  [a-c] and  $200 \text{ nm}$  [d-f]. (a) and (d) MCC gel, (b) and (e) MCC-xylan, (c)-(f) MCC-CMC.

crosslinker. In all of the FT-IR spectra, a broad peak in the range of  $1643\text{--}1654\text{ cm}^{-1}$  is observed. The peak is assigned to the HOH bending of the physically absorb water, since all the precursors and hydrogels are hygroscopic in nature [27]. However, the broad peak is also merged with the asymmetric stretching of  $\text{COO}^-$  which for CMC is in the range of  $1600\text{--}1620\text{ cm}^{-1}$  [17]. However, the asymmetric and symmetric stretching of  $\text{COO}^-$  are perceived to observe only in Figure 3c. The symmetric stretching of  $\text{COO}^-$  is reported  $1423\text{--}1446\text{ cm}^{-1}$  which is merged with the bending of  $-\text{CH}_2$  moiety at  $1454\text{ cm}^{-1}$  [28, 29]. The skeletal vibrations of C-C and C-O of pyranose ring are observed at  $1354\text{--}1363\text{ cm}^{-1}$ . A broad spectrum at  $1080\text{ cm}^{-1}$  is assigned as collective spectra of antisymmetric  $\beta\text{-(1}\rightarrow\text{4)}$  glycosidic linkage and C-C bending mode. The band at  $842\text{--}845\text{ cm}^{-1}$  is assigned as the glycosidic C-H deformation with ring vibration.

### 3.2. Morphology of hydrogels

The hydrogel morphology is visualized by FESEM and optical microscopy and represented in Figures 4 and 5 respectively. From the FESEM images, all gels are found to be coarse in nature with uneven surface. The coarse nature of hydrogels is also visible in optical microscope images. The uneven surface creates multilayered morphology of

hydrogel and thus pores are visible among layers. Further, the morphology of Cephalexin loaded gels is observed in optical microscope and is given in Figure 5d–f. The drug molecules appear to be within the green patches on the surface of the hydrogels. The distribution of drug is found to be uneven. The random distribution of drug molecules implies that various hydroxyl and carboxyl moieties make ionic bonds with the drug molecules.

### 3.3. Rheological behavior of hydrogel

Figure 6 represents the rheological behavior of the hydrogels. By varying the rate of shear between  $0.01\text{--}1000\text{ s}^{-1}$ , the viscosity of the gels is given in Figure 6a. With the increasing shear rate, we observe a decline in viscosity. The nature of the curves follows shear thinning behavior of the gels which is further confirmed by model fitting within a power-law model. Power law equation is given as,

$$\eta = m(\dot{\gamma})^{n-1} \quad (6)$$

Where,  $\dot{\gamma}$  is shear rate,  $\eta$  is viscosity,  $m$  is consistency index and  $n$  is power-law index. The fitted values of parameters are given in Table 1. Additionally the correlation coefficients ( $R^2$ ) are given in Table 1 which

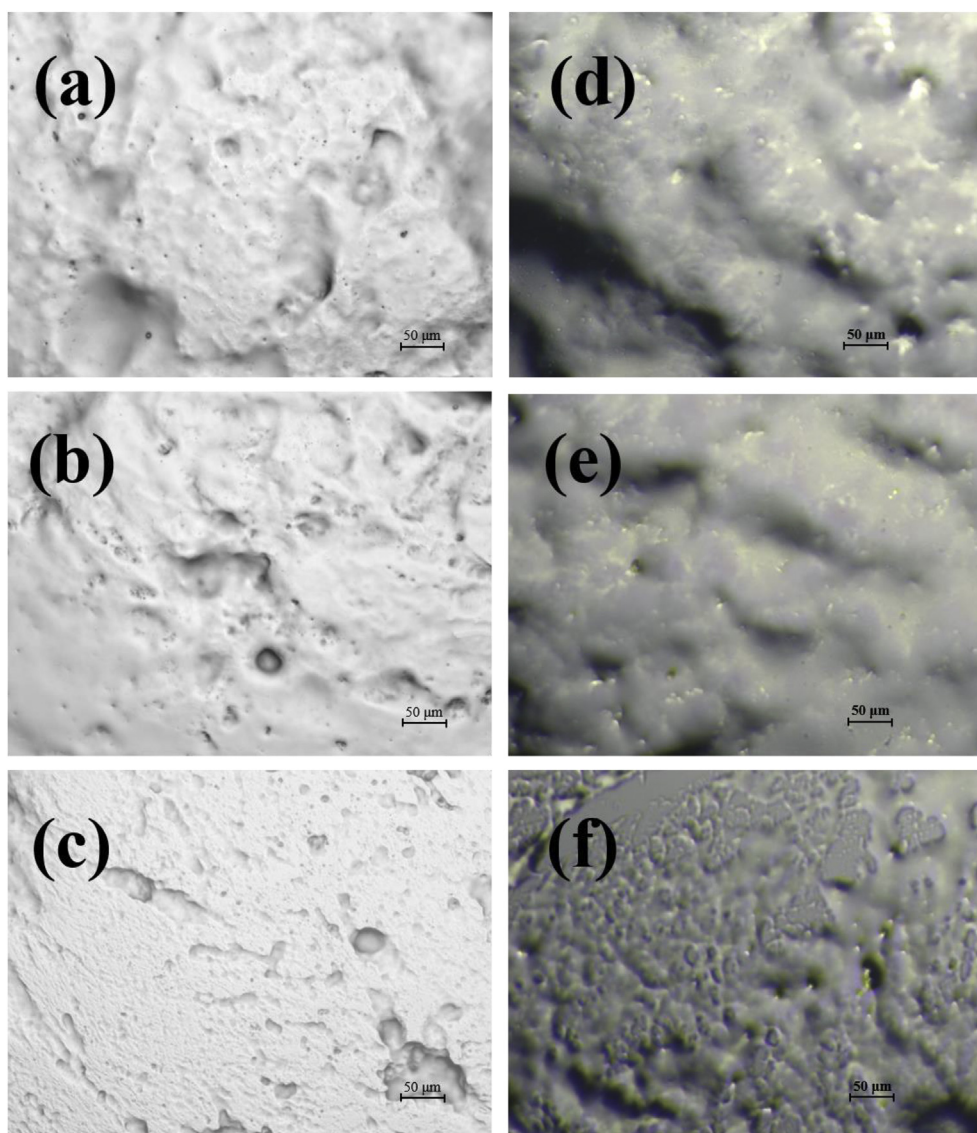


Figure 5. Optical microscope images of hydrogels (a–c) and Cephalexin loaded gels (d–f). (a) and (d) MCC gel, (b) and (e) MCC-xylan, (c)–(f) MCC-CMC.

represent the goodness of fit. The  $R^2$  values for all gels are greater than 0.95 which implies the power law model adequately represent the viscosity behavior within the given shear rate. The shear thinning nature of the hydrogels are mathematically confirmed by the power law index which is having lower values than unity. However, hydrogel is a cross-linked structure and the repeat unit of polysaccharide has long chain with higher molecular weight. Therefore, during the shear rate range from  $1 \times 10^{-2}$  to  $1 \times 10^{-1} \text{ s}^{-1}$ , the applied shear rate is very small and the cross-linked network resists the deformation. Hence, a broad peak at low shear rate is observed for all three gels. Further, the broad peak is stiffer for MCC-CMC than MCC-xylan, indicating the initial stiffness in the MCC-CMC gel compared to the other two gels. Later, we also observe that the viscosity of MCC-CMC is always higher by an order of ten when compared to the remaining hydrogels.

Further, we have also examined the viscoelastic properties of the gels by amplitude sweep test in Figure 6b by varying the strain from 0.1-1000%. It is observed that until the crossover point, storage modulus dominates over the loss modulus. For all three gels, crossover strain lies beyond 100%, reflecting the stability of crosslinked gels. We here observe that the copolymerized MCC-CMC and MCC-xylan gels can sustain higher deformation than MCC gel. From the amplitude sweep test, we further determine the LVR at 5% strain. The dominance of elastic response over viscous response is further examined in frequency sweep (Figure 6c) where the frequency is varied from 0.01-100 Hz and at a constant strain of 5%. From Figure 6c, we obtain the crossover point for MCC gel at 64 Hz. Although the crossover point of MCC-CMC exceeds when compared to MCC gel, MCC-xylan gel is seen to break early. Up to the crossover point, the elastic response dominates which is a desirable property for hydrogels. We further observe the enhancement of storage and loss moduli of MCC-CMC gel as compared to MCC gel whereas those are reduced for MCC-xylan gel.

**Table 1.** Power law parameters.

Name of the hydrogel	m	n	$R^2$
MCC gel	$2.74 \times 10^4$	0.414	0.99
MCC-xylan	$1.60 \times 10^4$	0.507	0.96
MCC-CMC	$1.44 \times 10^5$	0.442	0.99

Thereafter, we calculate the loss tangent from Eq. (1). The corresponding loss tangent vs frequency plot is given in Figure 7. The sol-gel transitions for MCC-CMC and MCC gel are observed after 64 Hz whereas MCC-xylan gel attains it after 20 Hz. A gradual increment of loss tangent is observed before the sol-gel transition. This is because with increasing frequency, the crosslinked structure starts losing the elastic nature.

### 3.4. Swelling study and gel fraction

The water absorbency by hydrogels is determined by swelling ratio. The degree of crosslinking is represented by gel fraction. The densely crosslinked hydrogel network has less flexibility to expand. Hence, it entraps lower amount of water and has lower swelling ratio. Here we have performed the swelling of hydrogels in AGF, AIF, PBS and DI water, keeping in mind the Cephalexin uptake and *in vitro* delivery in physiological buffers. Figure 8a represents the swelling ratio of hydrogels as calculated from Eq. (2). The order of swelling for DI water and buffers are found to be MCC-CMC > MCC-xylan > MCC gel.

For all three hydrogels, highest swelling is obtained with DI water and order of swelling is given by: DI water > PBS > AIF > AGF. Hydroxyl (MCC, xylan and CMC) and carboxymethyl moieties (CMC) are dominant charged species of hydrogels. For that, the electrostatic repulsion of the moieties in the side chain of pyranose ring cause swelling. Thus having

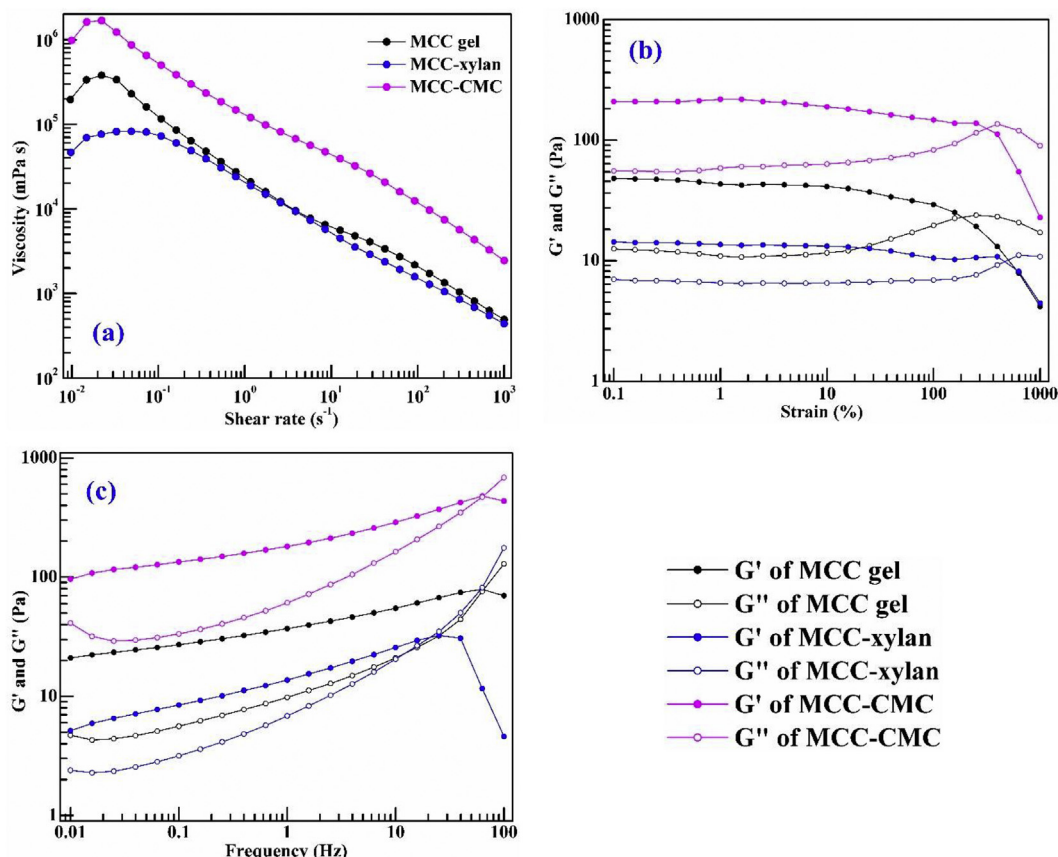


**Figure 6.** Rheology of hydrogels. (a) Viscosity, (b) amplitude sweep, (c) frequency sweep.



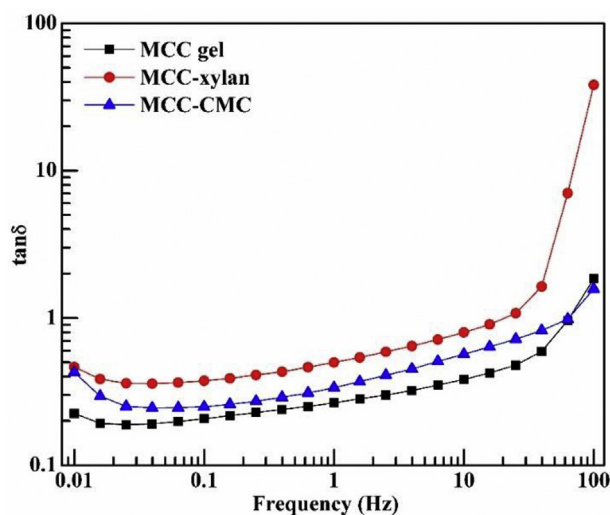


Figure 7. Loss tangent of hydrogels.

been in the ion free medium of DI water, the hydrogels swell more than in the buffers. The ionic moieties of hydrogels are readily saturated with free ions of buffers causing less repulsion and less amount of swelling. Further the longer carboxymethyl moiety of CMC gives MCC-CMC network a higher flexibility, resulting in higher swelling over the other two hydrogels. The calculated gel fraction, given in Figure 8b, follows the reverse trend of swelling i.e. MCC gel has a highest gel fraction of 96.98% among all the three hydrogels. Gel fraction here represents the degree of crosslinking. With the increase in crosslinking lower swelling is observed because of less flexibility of crosslinked chains to expand.

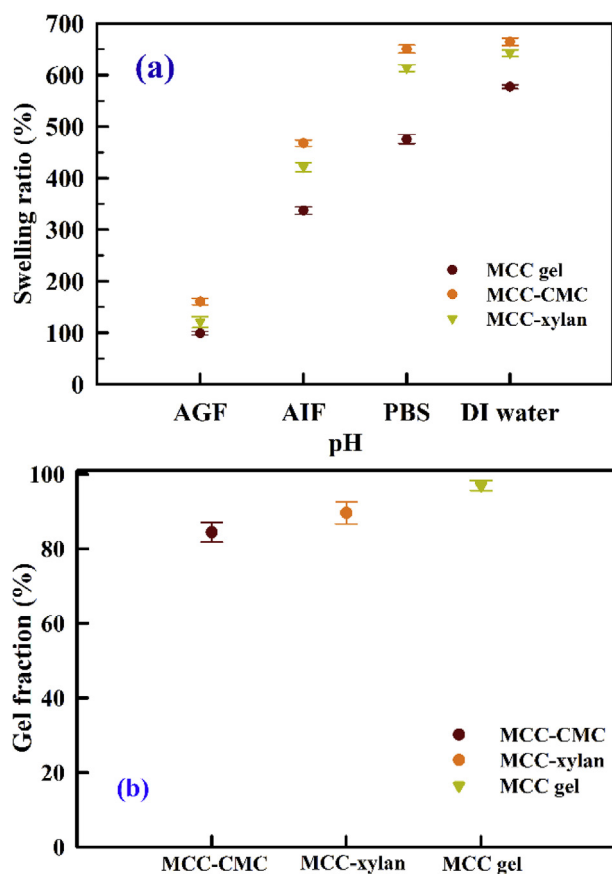


Figure 8. (a) Swelling ratio of hydrogels in DI water and various buffers. (b) Gel fraction of hydrogels.

### 3.5. Loading and *in vitro* release of Cephalexin

The loading of MCC gel has been recorded as 19.64% ( $\pm 0.56\%$ ) whereas copolymerized MCC-CMC and MCC-xylan have loading of 26.48% ( $\pm 1.15\%$ ) and 24.25% ( $\pm 0.91\%$ ) respectively. The higher amount of drug loading in MCC-CMC can be attributed to the higher swelling ratio of hydrogel. Barkhordari and Yadollahi reported 0.061 gm of Cephalexin incorporated into per gm of layer double hydroxide – Cephalexin nanohybrid with CMC as protective capsule [14]. Therefore, only 6.1% of loading of Cephalexin is recorded from their reported method. However, they have considered  $0.6 \text{ mg mL}^{-1}$  concentration of drug for the loading. The *in vitro* delivery of Cephalexin at three simulated body fluids, namely; AGF, AIF and PBS are performed for 8 h and given in Figure 9a–c. Further Figure 9d represents the *in vitro* delivery in successive physiological buffers i.e. at AGF for 2 h, followed by AIF for 2 h and subsequently in PBS for 6 h. The mean emptying time in stomach is noted as 1.08 h ( $\pm 0.11$  h), followed by the transit time in small intestine as 1.75 h ( $\pm 0.25$  h) which leaves the arrival time in colon is 2.83 h ( $\pm 0.33$  h) [30]. Therefore, the above mentioned *in vitro* release study in successive buffers (Figure 9d) would be sufficient to simulate the release profile in gastrointestinal tract. This will elucidate the efficiency of MCC based hydrogels as an effective carrier for Cephalexin. Further, the pH and composition of AGF, AIF and PBS adequately represent the body fluids inside stomach, small intestine and colon respectively.

The *in vitro* release in AGF produces 14–16% delivery of drug whereas higher delivery of 83–87% and 87–98% are observed in AIF and PBS respectively. The higher amount of release in AIF and PBS are attributed to the high degree of swelling of hydrogels. At pH 1.2, higher amount of  $\text{H}^+$  ions are available to protonate the hydroxyl moieties which negates the lower electrostatic repulsion causing lower swelling. Due to the lower swelling, less free path is created to let the Cephalexin diffuse in buffer. However, burst release is observed in AIF and PBS for the first 2 h. At higher pH, deprotonated hydroxyl moieties repel each other causing higher swelling and greater diffusion of drug into the media. After 2 h, release rate in PBS becomes higher than that in AIF media because of the various ions in PBS when compared to AIF. However, in literature, Barkhordari and Yadollahi reported the cumulative release of drug is 10% in AGF for 2 h followed by 60% in AIF for 2 h and by 22% in PBS for 4 h [14]. Further, the kinetic mechanism is reported as ion-exchange process followed by the diffusion of Cephalexin into the aqueous medium. Tomić et al. reported the *in vitro* release of Cephalexin in PBS (pH = 7.4) at  $37^\circ\text{C}$  from the 2-hydroxyethyl methacrylate, itaconic acid and poly (alkylene glycol) methacrylates based hydrogel. The hydrogel releases less than 80% of drug within 10 h and  $\sim 100\%$  release after 90 h [16]. Further, steady release of drug is observed after the initial burst release.

Figure 9d represents the *in vitro* delivery of Cephalexin in successive buffers. The cumulative release in AGF for first 2 h resembles the trend of the release in pure AGF. However, the burst release is prevented when the hydrogels are dipped into AIF and PBS buffer respectively because of the already protonated functional moieties of hydrogel. Further, after 4 h (2 h in AGF and 2 h in AIF), the amount of drug release is 45–54%, which is higher than the *in vitro* release in pure AIF buffer. We did not observe any significant drug release after 8 h for the release in individual buffers (Figure 9a–c). But in sequential release, PBS is able to extract  $\sim 45\%$  of drug from hydrogels making the cumulative release to 91–98%. Hence, it is concluded that MCC based hydrogels can facilitate the delivery of Cephalexin to 8–9% in stomach, 37–45% in the small intestine and 37–44% in the colon only when the hydrogels are first exposed to AGF. For the oral delivery route, the carrier will not remain in the gastrointestinal tract for prolong period as reported by Tomić et al., rather a higher amount of drug release is necessary within a stipulated period. Therefore, a cumulative release of 87–98% in PBS within 8 h elucidates the effectiveness of MCC based hydrogels as an effective carrier of Cephalexin.

Figure 9 also draws a comparative study of *in vitro* delivery profile of Cephalexin among MCC, MCC-xylan and MCC-CMC gel. The release of



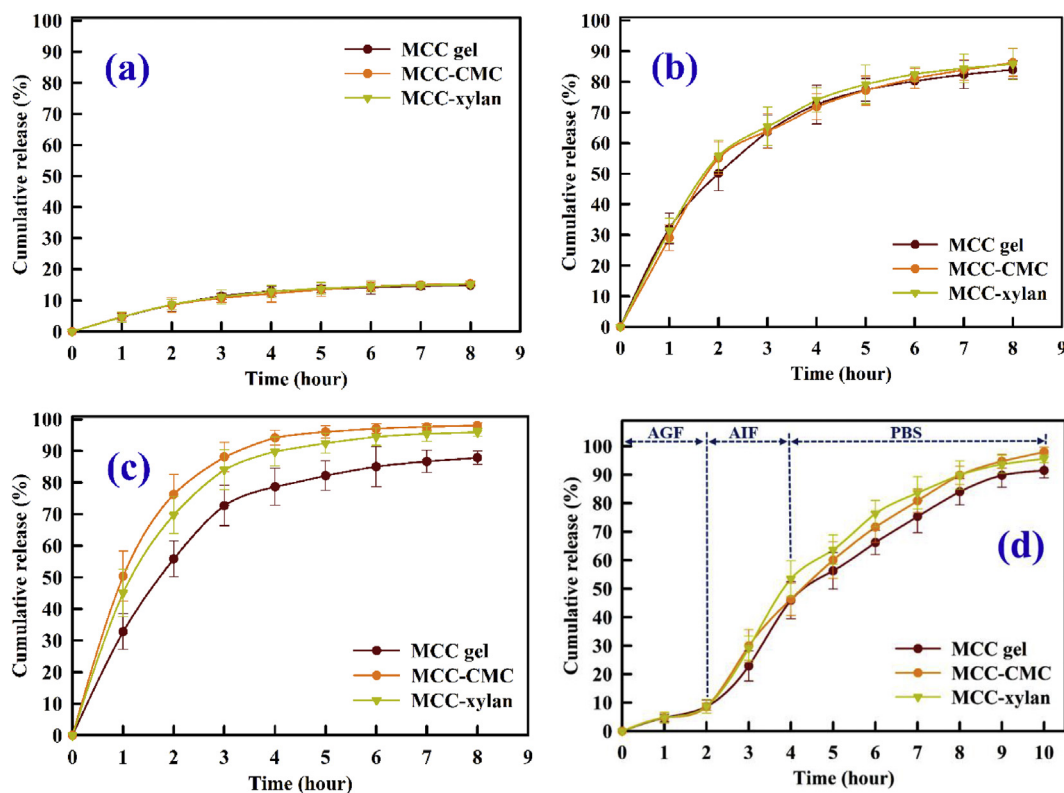


Figure 9. *In vitro* release of Cephalexin in physiological buffers. (a) AGF buffer, (b) AIF buffer, (c) PBS buffer, (d) AGF-AIF-PBS buffers.

drug in independent buffers primarily depends on the swelling of the gels. Hence, it is expected to have higher release rate from MCC-CMC gel as it consistently produces higher swelling ratio than the other two gels. Further, MCC-CMC hydrogel has an additional carboxyl moiety along with hydroxyl moieties which provide greater number of binding sites for drug. Hence, the sites facilitate affinity towards the cations in buffer and release the drug after the initial burst release. Thus the order of release is MCC-CMC > MCC-xylan > MCC gel for all buffer mediums.

The lower amount of Cephalexin release in AGF followed by the accelerated release in AIF and PBS, can also be attributed to the existence of the drug at various forms. The presence of  $-\text{COOH}$ ,  $-\text{CONH}$ ,  $-\text{NH}_2$  moieties in the Cephalexin molecule and its inherent acid-base properties resemble to the dipeptide molecule. Depending upon the pH of aqueous medium, Cephalexin (denoted as CPX) can exist as cation ( $\text{H}_2\text{CPX}^+$ ), zwitterion ( $\text{HCPX}^\ominus$ ) and anion ( $\text{CPX}^\ominus$ ) [31]. The zwitterion form of Cephalexin dominates within a pH range of 2.56–6.88 [32]. Cephalexin is anionic above pH 6.88 and is cationic below 2.56 [14]. Below pH 2.56, the drug exists in cationic form which is repelled by the excess  $\text{H}^+$  ions present in AGF medium. This prevents higher amount of release of drug in AGF. However, in zwitterion form, the drug exhibit both acidic and basic properties. Therefore, it can combine with the metal ions and  $\text{H}^+$  ions in AIF, resulting in a higher release of drug. Further, in the anionic form (above 6.88 pH), the Cephalexin can bind with the available metal ions in PBS buffer. For this to happen, the initial burst release of Cephalexin is higher in PBS as compared to the *in vitro* release in AIF. For the same reason, PBS buffer facilitates extraction of Cephalexin in AGF-AIF-PBS buffer system.

#### 4. Conclusions

MCC based homopolymerized gel and copolymerized gels with CMC and xylan are synthesized using EGDE crosslinker. MCC-CMC gels has swelling ratio of 160%, 468%, 651% and 664% in AGF, AIF, PBS and DI water respectively which are higher among three gels in the respective

mediums. The swelling ratio is shown to increase with the pH. The gel fraction produces the reverse trend of swelling ratio whereby the highest gel fraction of 96.98% is obtained for MCC gel. A coarse nature is observed in the morphological observation for all hydrogels. Further, the hydrogels follow shear thinning behavior with increasing shear rate. A longer gel point at 64 Hz is observed for MCC-CMC hydrogel, whereas MCC-xylan produces a shorter gel point of 20 Hz. Up to the gel point, elastic nature of hydrogel prevails as determined from the loss tangent. The longer gelation point of MCC-CMC reflects the suitability of MCC-CMC among three gels. Further MCC-CMC gel shows a drug loading capacity of 26.48% ( $\pm 1.15\%$ ) which is highest among the three gels. Further, MCC-CMC releases 15% Cephalexin in AGF, 86% in AIF and 98% in PBS respectively. The *in vitro* release kinetics in AIF and PBS reveal initial burst release of Cephalexin due to the swelling of gels followed by a steady release.

#### Declarations

##### Author contribution statement

Debashis Kundu: Conceived and designed the experiments; Performed the experiments; Analyzed and interpreted the data; Contributed reagents, materials, analysis tools or data; Wrote the paper.

Tamal Banerjee: Conceived and designed the experiments.

##### Funding statement

This research did not receive any specific grant from funding agencies in the public, commercial, or not-for-profit sectors.

##### Competing interest statement

The authors declare no conflict of interest.

### Additional information

No additional information is available for this paper.

### Acknowledgements

The authors acknowledge the Analytical Laboratory, Department of Chemical Engineering and the Central Instrument Facility of the Indian Institute of Technology Guwahati for providing the characterization instruments used in this work.

### References

- [1] H. Zhu, W. Luo, P.N. Ciesielski, Z. Fang, J.Y. Zhu, G. Henriksson, M.E. Himmel, L. Hu, Wood-derived materials for green electronics, biological devices, and energy applications, *Chem. Rev.* 116 (2016) 9305–9374.
- [2] D. Trache, M.H. Hussin, C.T. Hui Chuin, S. Sabar, M.R.N. Fazita, O.F.A. Taiwo, T.M. Hassan, M.K.M. Haafiz, Microcrystalline cellulose: isolation, characterization and bio-composites application—a review, *Int. J. Biol. Macromol.* 93 (2016) 789–804.
- [3] X. Shen, J.L. Shamshina, P. Berton, G. Gurau, R.D. Rogers, Hydrogels based on cellulose and chitin: fabrication, properties, and applications, *Green Chem.* 18 (2016) 53–75.
- [4] F. Ullah, M.B.H. Othman, F. Javed, Z. Ahmad, H.M. Akil, Classification, processing and application of hydrogels: a review, *Mater. Sci. Eng. C* 57 (2015) 414–433.
- [5] D. Choe, Y.M. Kim, J.E. Nam, C.S. Shin, Y.H. Roh, Synthesis of high-strength microcrystalline cellulose hydrogel by viscosity adjustment, *Carbohydr. Polymers* 180 (2018) 231–237.
- [6] X. Liang, B. Qu, J. Li, H. Xiao, B. He, L. Qian, Preparation of cellulose-based conductive hydrogels with ionic liquid, *React. Funct. Polym.* 86 (2015) 1–6.
- [7] H. Hu, J. You, W. Gan, J. Zhou, L. Zhang, Synthesis of allyl cellulose in NaOH/urea aqueous solutions and its thiol-ene click reactions, *Polym. Chem.* 6 (2015) 3543–3548.
- [8] S. Sood, V.K. Gupta, S. Agarwal, K. Dev, D. Pathania, Controlled release of antibiotic amoxicillin drug using carboxymethyl cellulose-cl-poly(lactic acid-co-itaconic acid) hydrogel, *Int. J. Biol. Macromol.* 101 (2017) 612–620.
- [9] N.M.L. Hansen, D. Plackett, Sustainable films and coatings from hemicelluloses: a review, *Biomacromolecules* 9 (2008) 1493–1505.
- [10] X.-W. Peng, J.-L. Ren, L.-X. Zhong, F. Peng, R.-C. Sun, Xylan-rich “Hemicelluloses-graft-acrylic acid ionic hydrogels with rapid responses to pH, salt, and organic solvents, *J. Agric. Food Chem.* 59 (2011) 8208–8215.
- [11] X.-F. Sun, H.-H. Wang, Z.-X. Jing, R. Mohanathas, Hemicellulose-based pH-sensitive and biodegradable hydrogel for controlled drug delivery, *Carbohydr. Polym.* 92 (2013) 1357–1366.
- [12] X.-F. Sun, Z. Gan, Z. Jing, H. Wang, D. Wang, Y. Jin, Adsorption of methylene blue on hemicellulose-based stimuli-responsive porous hydrogel, *J. Appl. Polym. Sci.* (2015) 132.
- [13] D. Dax, M.S. Chávez, C. Xu, S. Willför, R.T. Mendonça, J. Sánchez, Cationic hemicellulose-based hydrogels for arsenic and chromium removal from aqueous solutions, *Carbohydr. Polym.* 111 (2014) 797–805.
- [14] S. Barkhordari, M. Yadollahi, Carboxymethyl cellulose capsulated layered double hydroxides/drug nanohybrids for cephalixin oral delivery, *Appl. Clay Sci.* 121–122 (2016) 77–85.
- [15] M.S. Legnoverde, S. Simonetti, E.I. Basaldella, Influence of pH on cephalixin adsorption onto SBA-15 mesoporous silica: theoretical and experimental study, *Appl. Surf. Sci.* 300 (2014) 37–42.
- [16] S.L. Tomić, M.M. Babić, K.M. Antić, J.S. Jovasević Vuković, N.B. Malesić, J.M. Filipović, pH-sensitive hydrogels based on (meth)acrylates and itaconic acid, *Macromol. Res.* 22 (2014) 1203–1213.
- [17] H. Kono, K. Onishi, T. Nakamura, Characterization and bisphenol A adsorption capacity of  $\beta$ -cyclodextrin-carboxymethylcellulose-based hydrogels, *Carbohydr. Polym.* 98 (2013) 784–792.
- [18] D. Kundu, S.K. Mondal, T. Banerjee, Development of  $\beta$ -cyclodextrin-cellulose/hemicellulose based hydrogels for the removal of Cd (II) and Ni (II): synthesis, kinetics and adsorption aspects, *J. Chem. Eng. Data* 64 (2019) 2601–2617.
- [19] L. Zhang, L.L. Li, N.J. Liu, H.L. Chen, Z.R. Pan, S.J. Lue, Pervaporation behavior of PVA membrane containing  $\beta$ -cyclodextrin for separating xylene isomeric mixtures, *AIChE J.* 59 (2013) 604–612.
- [20] J.F. Almeida, A. Fonseca, C.M.S.G. Baptista, E. Leite, M.H. Gil, Immobilization of drugs for glaucoma treatment, *J. Mater. Sci. Mater. Med.* 18 (2007) 2309–2317.
- [21] J. Zhou, L. Zhang, Q. Deng, X. Wu, Synthesis and characterization of cellulose derivatives prepared in NaOH/Urea aqueous solutions, *J. Polym. Sci., Part A: Polym. Chem.* 42 (2004) 5911–5920.
- [22] X. Gao, Y. Cao, X. Song, Z. Zhang, X. Zhuang, C. He, X. Chen, Biodegradable, pH-responsive carboxymethyl cellulose/poly(acrylic acid) hydrogels for oral insulin delivery, *Macromol. Biosci.* 14 (2014) 565–575.
- [23] S.M. Alshehri, A. Aldalbahi, A.B. Al-hajji, A.A. Chaudhary, M.I.H. Panhuis, N. Alhokbany, T. Ahmad, Development of carboxymethyl cellulose-based hydrogel and nanosilver composite as antimicrobial agents for UTI pathogens, *Carbohydr. Polym.* 138 (2016) 229–236.
- [24] B.Y. Swamy, Y.-S. Yun, In vitro release of metformin from iron (III) cross-linked alginate-carboxymethyl cellulose hydrogel beads, *Int. J. Biol. Macromol.* 77 (2015) 114–119.
- [25] D. Kundu, T. Banerjee, Carboxymethyl cellulose-xylan hydrogel: synthesis, characterization and *in vitro* release of Vitamin B<sub>12</sub>, *ACS Omega* 4 (2019) 4793–4803.
- [26] M. Sekkal, V. Dincq, P. Legrand, J.P. Huvenne, Investigation of the glycosidic linkages in several oligosaccharides using FT-IR and FT Raman spectroscopies, *J. Mol. Struct.* 349 (1995) 349–352.
- [27] X.F. Sun, R.C. Sun, P. Fowler, M.S. Baird, Isolation and characterization of cellulose obtained by a two-stage treatment with organosolv and cyanamide activated hydrogen peroxide from wheat straw, *Carbohydr. Polym.* 55 (2004) 379–391.
- [28] I. Ahemen, O. Meludu, E. Odoh, Effect of Sodium Carboxymethyl cellulose concentration on the photophysical properties of zinc sulfide nanoparticles, *Br. J. Appl. Sci. Technol.* 3 (2013) 1228–1245.
- [29] Y. Yin, L. Berglund, L. Salmén, Effect of steam treatment on the properties of wood cell walls, *Biomacromolecules* 12 (2011) 194–202.
- [30] Y.S.R. Krishnaiah, S. Satyanarayana, Y.V. Rama Prasad, S. Narasimha Rao, Gamma scintigraphic studies on guar gum matrix tablets for colonic drug delivery in healthy human volunteers, *J. Control. Release* 55 (1998) 245–252.
- [31] V.G. Alekseev, A.A. Nikiforova, S.V. Markelova, Reaction of Cefalexine with manganese (II), cobalt (II), nickel (II), zinc (II), and cadmium (II) ions, *Russ. J. Gen. Chem.* 76 (2006) 1468–1470.
- [32] G. Nazari, H. Abolghasemi, M. Esmaeili, Batch adsorption of cephalixin antibiotic from aqueous solution by walnut shell-based activated carbon, *J. Taiwan Inst. Chem. Eng.* 58 (2016) 357–365.